stretch of homology between adenoviral vector and packaging cell line can give rise to cytopathic effect-inducing, helper-dependent E1-positive particles. Hum Gene Ther 13：909-920, 2002

20) Fallaux FJ, Bout A, van der Velde I, van den Wollenberg DJ, Hehir KM, Keegan J, Auger C, Cramer SJ, van Ormondt H, van der Eb AJ, Valerio D,Hoeben RC：New helper cells and matched early region 1-deleted adenovirus vectors prevent generation of replication-competent adenoviruses. Hum Gene Ther 9：1909-1917, 1998

21) Aghi M,Martuza RL：Oncolytic viral therapies - the clinical experience. Oncogene 24：7802-7816, 2005

22) Lin E,Nemunaitis J：Oncolytic viral therapies. Cancer Gene Ther 11：643-664, 2004

23) Ries SJ,Brandts CH：Oncolytic viruses for the treatment of cancer：current strategies and clinical trials. Drug Discov Today 9：759-768, 2004

24) 厚生労働省医薬局長通知：細胞・組織利用医薬品等の取扱い及び使用に関する基本的考え方. 医薬発第266号, 平成13年3月28日

25) 厚生労働省医薬局長通知：ヒト由来細胞・組織加工医薬品等の品質及び安全性の確保に関する指針. 医薬発 第1314号, 平成12年12月26日

26) 厚生労働省医薬局長通知：ヒト幹細胞を用いる臨床研究に関する指針の施行等について ヒト幹細胞を用いる臨床研究. 健発第0703003号, 平成18年7月3日

27) EMEA：Point to consider on xenogenic cell therapy medicinal products. 2003.12.17

28) EMEA：Point-to-consider on the manufacture and quality control of human somatic cell therapy medicinal products. CPMP/BWP/41450/98, 2001.5.31

29) FDA/CBER：Suitability determination for donors of human cellular and tissue-based products. 97N-484S, 1999.9.30

30) 厚生労働省医薬局長通知：生物由来製品及び特定生物由来製品の指定並びに生物由来原料基準の制定等について. 医薬発第052001号, 平成15年5月20日

ファルマシア

別刷

社団法人
日本薬学会
The Pharmaceutical Society of Japan

多形現象を示す医薬品の製剤化における速度論的安定性評価
温度・湿度及び光の影響を中心として

松田芳久
Yoshihisa MATSUDA
神戸薬科大学教授

1 はじめに

医薬品製剤は最終剤形のいかんを問わず，これらを構成する原薬は固体状態である場合が大半を占めているが，原薬の結晶特性や粉体物性が製剤工程の円滑性や製品の品質特性，さらには薬効発現のしかたにも少なからぬ影響を及ぼすことが知られている．このような状況に加えて行政当局による指導も反映し，近年，製薬企業の製剤研究者を中心として，原薬の結晶形への関心とその取扱いの重要性に対する認識が急速に深まっている．したがって，製剤開発の源流に位置するプレフォーミュレーション(予備処方設計)過程で原薬の結晶特性を十分に把握した上で，これらの情報に基づいた合理的な製剤設計を行うことは，製剤の品質向上を図るために極めて重要である．

本稿では製剤工程で遭遇する問題点を想定しながら，筆者らの研究において得られた成果を中心に，多形現象を示す医薬品の結晶転移における安定性について基礎的観点から概説する．

2 結晶形をめぐる最近の話題

最近，関係者の大きな関心を集めた結晶形に関する主なトピックスとして，以下の例が挙げられる．1つは消化性潰瘍治療薬ファモチジンB型結晶に関する特許紛争である．本訴訟では先発メーカーが2種類の結晶多形A型とB型が存在するファモチジンに関する物質特許を有していたにも関わらず，同社の製品ではB型結晶を採用していたことが原因となった．その後，外国の後発メーカーに「B型結晶製造」の特許を取得され，先発メーカーが後発メーカーから特許の実施許諾を受けることによって製造を継続している．これは，“公知の化合物でも結晶形が公知の化合物と異なり，安定性や吸収性が改善されたなどの有利な性質を持つ場合は，そのことだけで「新しい物理的状態Xを有する化合物Y」という特許を取得することが可能である”という，特許取得における流れの変化を背景としている．なお，このほかにも結晶形に関する最近の係争例として，ラニチジン，ニカルジピンなどがある．

一方，製造中止の例として，抗HIV薬であるリトナビル(アボット社)の事例が挙げられる．[1,2] この薬物には現在までに5種類の結晶形が存在することが明らかにされているが，1996年に発売された当時は結晶多形の存在は明らかにされていなかった．しかし発売2年後に同社で最も安定な結晶形が出現し，溶解性が規格範囲外まで低下したために製造が中止され，2000年にこの安定形結晶による新しい剤形で再申請せざるを得なくなるという事態に陥った．

これらの事例は，いずれも製剤開発では最適な結晶形の選択が重要なキーポイントとなることを如実に示している．

3 結晶多形とは

化学的組成は同じであっても結晶構造の異なるものを多形という．最近では医薬品の80%に結晶多形が存在するといわれており，[3] 結晶形の違いは溶解度，溶解速度などの物理化学的性質や化学的安定性にも影響を及ぼす．多形は結晶内部での分子配列やコンフォメーションの違いによって生じるが，熱力学的に最も安定な結晶形を安定形，これよりも不安定な結晶形をすべて準安定形という．準安定形は複数個存在する場合が多く，5種類以上に及ぶこともある．また，結晶の構成成分が単一成分である場

合を多形，水和物や溶媒和物のように2成分以上の場合を擬似多形として取り扱うが，例えば，利尿薬であるフロセミドには非晶質も含めて7種類の結晶形が存在する.[4] 安定形結晶は多形の中で一般に溶解度は最も低い．これに対して準安定形は安定形より格子エネルギーが小さいので，より高い溶解度を示す．最近，これまでに論文中で報告された81の医薬品化合物の溶解度に着目した研究では，安定形に対する準安定性結晶の溶解度比は，大半は5倍以下であるが，なかには23倍にも及ぶ特異な化合物もあることが報告されている.[5] したがって，難溶性医薬品の固形製剤を設計する場合に準安定形をうまく利用すれば，バイオアベイラビリティを改善することが期待される．しかし準安定形結晶はこのような優れた溶解特性を示す反面，安定形へ転移するため，溶解特性が低下する恐れがあることがこれまでに指摘されてきた．このため，現在ICH(日米EU医薬品規制調和国際会議)において議論が進められているQ8(Pharmaceutical Development)でも，原薬に関する記載については製剤の性能・製造性に影響する物理的・化学的・生物学的特性及び特別に設計された特性(固体状態での特性など)を特定し，考察することが推奨されている．

4 固形製剤の製剤工程における結晶多形の取扱い

固形製剤の製剤特性を長期間にわたって安定した状態に維持するためには，原薬結晶の品質管理は極めて重要である．しかし，これまでに報告された多形に関する論文の大半は粉末X線回折測定や熱分析に基づいた結晶学的パラメータや溶解性に関する議論であり，また安定性の面から準安定形結晶の転移に着目した研究であっても，その大多数は定性的な取扱いに留まっている．転移現象の定量的体系化を阻む要因として，転移が不均一系反応であることに加えて，関係する因子が複雑に絡み合っていることによる．このため，筆者らの研究[6]に端を発する，固体反応速度論に基づいた転移現象の解析が本格的に展開されるまでは，外国の専門書においても転移に関しては単に"sooner or later"という曖昧な表現しかなされておらず，その実態については全く記述されていなかったのは，上記の事情を反映しているものと考えられる．

ところで，以下に示すような湿式顆粒圧縮法による代表的な固形製剤工程では，各工程中で結晶は種々のストレス(機械的外力，熱，水分，光など)を受けるが，製剤の適切な品質保証を行う上で，結晶がこれらの因子に対してどのような挙動を示すかをあらかじめ明らかにしておく必要がある．以下に幾つかの事例を挙げる．

[原薬] →(粉砕)→(混合)→(練合)→(造粒)→(乾燥)→(製錠)→[錠剤]

1. 粉砕による結晶転移

粉砕機内では結晶に大きな機械的エネルギーが加えられ，同時に発生する摩擦熱によって転移や非晶質化が起こる可能性がある．粉砕に伴う転移は，結晶の変形や破砕によって結晶内部に多くの歪みが生じ，結晶構造が変化するためである．遠心ボールミルによるニメタゼパムの粉砕では，安定形(Ⅰ)と準安定形(Ⅱ)は，いずれも粉砕エネルギーの増加(粉砕機の回転速度の増加)に伴って非晶質化が速やかに進行したが，Ⅰ形は残存率20%で平衡状態に達したのに対して，Ⅱ形はいったん完全に非晶質化した後，再びⅠ形へ転移するという，異なった転移様式を示した(図1)．これらの転移過程は，前者の場合ではJander式で整理できたのに対して，後者はみかけの1次反応で進行した．これらの結晶形は，瞬間的な衝撃粉砕機構に基づくピンミル中では全く

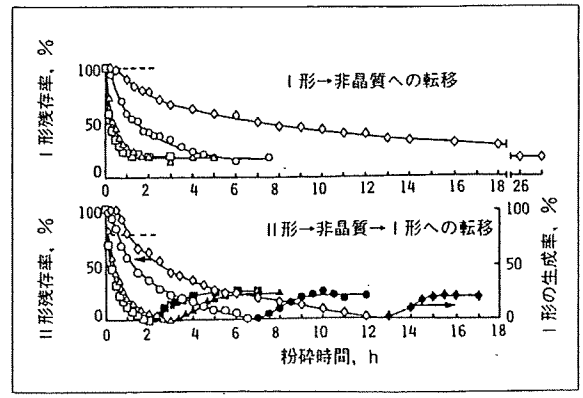

図1 ボールミル粉砕中のニメタゼパムⅠ形及びⅡ形結晶の結晶性の経時変化

回転速度：◇ 225 rpm；○ 270 rpm；△ 360 rpm；□ 450 rpm.

転移しないか又はほとんど転移しなかった(図1中の破線)．粉砕機構が異なると粉砕中に結晶内部に蓄積されたエネルギー量も異なるので，転移を起こしやすい結晶を長時間にわたって粉砕する場合には，機種の選定や運転条件の設定には十分に注意する必要がある．この場合，ジュール・トムソン効果が期待されるジェットミルは最適であろう．

2．造粒前後の工程における結晶転移

湿式造粒では練合の際に結合剤溶液が結晶と接触することにより，溶媒の影響によって転移を生じることがある．カルバマゼピンⅠ形結晶を，ヒドロキシプロピルセルロースを結合剤とする3種類の溶液(水，水/エタノール混液，エタノール)を用いて押し出し造粒したところ，水又はエタノールを用いて調製した顆粒では転移は起こらなかったが，混合溶媒の場合には練合・造粒中に2水和物に転移した．[7] また，同じ薬物について同じ結合剤の水溶液を用いた転移現象では，転移開始までの誘導期は水溶液の動粘度に比例して延長し，開始後の転移速度は逆に低下した．[8] これらの結果から，結合剤溶液の添加濃度や粘度は造粒性や製造された顆粒物性に密接に関係するのみならず，造粒中での多形転移にも少なからぬ影響を及ぼすことが示された．さらに前記と同じ3種類の溶媒系(結合剤なし)において撹拌・懸濁させたメフェナム酸Ⅱ形結晶(準安定形)は，いずれの溶媒中においても同じ転移機構に従ってⅠ形(安定形)へ転移したが，エタノール中では核形成過程における速度定数は温度に関わらず一定であったのに対して，核成長過程では温度の上昇に伴って増加した．これに対して混合溶媒系及び水系では，いずれの過程においても速度定数は温度に依存して変化した．[9]

一方，造粒後の乾燥工程においても加熱による転移の促進は当然起こり得る．例えば，噴霧乾燥造粒法によって顆粒を調製する場合は装置内で造粒と乾燥が同時に進行し，噴霧された薬物溶液の液滴が瞬間的に乾燥されるため，一般にはフロセミド[10]のように乾燥温度の高低に関わらず造粒品は非晶質化することが多いが，フェニルブタゾン[11]のように乾燥温度に依存して，非晶質化せずに複数の結晶形が生成することもある．

3．製錠中での結晶転移

圧縮成形における留意点は，各結晶形の中でいずれの結晶形が最も成形性に優れているかということに加えて，その結晶形が準安定形である場合には圧縮中に転移を起こす可能性がないかということである．前述のフロセミドでは2種類の準安定形(Ⅱ形とⅢ形)のうち，Ⅱ形は低圧縮力でも容易にⅠ形(安定形)へ転移するという，極めて特異な結晶形であることが判明した．また，圧縮特性についても結晶形間で相違が認められ，これらは圧縮後の応力緩和現象におけるレオロジー特性や錠剤硬度にも反映した．すなわちⅡ形は錠剤機の臼中から放出された後，著しい打錠障害を起こした．

5 製造後の保存時安定性

1．光に対する安定性

光に対して不安定な医薬品で，かつこれが多形現象を示す場合は外観変化(着色，変色)などの物理化学的変化と，分解などの化学的変化の両面から検討する必要があるが，光安定性に着目した研究例は極めて少ない．

フロセミドⅠ形(安定形)は過酷照射条件下でもほとんど着色せず，外観的には安定であったが，他の結晶形や溶媒和物は著しく着色し，かつ結晶間で有意な相違が認められた．[4] 筆者らによって確認されたこのような結晶形間での光安定性の相違に着目して，Villiers ら[12]はフロセミドの光分解に核形成及び核成長過程からなる固体反応モデルを適用して解析した結果，Ⅰ形とⅡ形の間で速度論的パラメータにおいて明確な差異を認めている．このほかに筆者らは，クエン酸タモキシフェンについても光安定性の相違を確認している．[13] 一方，カルバマゼピンの3種類の結晶形については，光照射によっていずれも少なくとも2種類の分解物が生成することを確認した．そこでこれらの結晶を圧縮成形した試料について光照射後のFT-IR正反射スペクトルを測定し，得られたデータに基づいて2次元的残存率の経時変化を比較したところ，いずれの結晶形も誘導期を伴うみかけの1次反応過程に従って減少し，かつ結晶間で顕著な相違を示した．[14] さらに塩酸ニカルジピンの2種類の結晶形(α形，β形)について同じ手法

により得られた2次元的残存率の経時変化は，結晶間で明確な相違を示したが，結晶を粉砕してほぼ非晶質状態となった両者を比較すると，この差異は一層拡大され，β形の光安定性は顕著に低下した.[15] これらの結果は，結晶性が低下するほど熱力学的にも光化学的にも不安定となることを明確に示している．したがって，粉砕処理後の原薬についても安定性を評価しておくことは重要である．なお，多形現象を示す医薬品の光安定性に関する詳細な解説については，別報[16]をご参照いただきたい.

2．温度及び湿度に対する安定性

前述のフロセミドⅢ形は圧縮に対しては十分に安定であったが，温度・湿度に対しては敏感で，60℃，100% RHでは半減期はわずか70分であった(図2)．ところが50% RHでは60℃という高温であっても，3か月後にわずか10%しか転移しなかった．吸湿等温線を他の結晶形と比較すると，Ⅲ形は水分子の吸着能が特に顕著であった．このように結晶表面に吸着した水分子が転移において触媒的な役割を果たすケースは多い．なお，これらの転移率曲線に固体反応式を適用して算出された誘導期と転移速度定数の間には，温度・湿度のいかんに関わらず密接な関係が成立した(図3)．この結果は誘導期が延長するほど，転移開始後の速度もこれに連動して緩慢になることを明確に示している．このような関係は他の転移系においても多数確認している．ところで，相対湿度から換算した絶対湿度に対して誘導期と転移速度定数をプロットし直すと，図4のようになる．これらの結果は，いずれのパラメータも温度のいかんに関わらず絶対湿度によって一義的に定まることを示唆している．また，絶対湿度0 g/m³においてすべての温度におけるデータの外挿点はY軸上の1点に収束した．この結果は，転移は温度のいかんに関わらず完全な乾燥条件下では起こり得ないことを強く示唆しており，保存時における原薬や製剤中の水分管理の重要性が理解できる.

吸湿性が極めて強いバルプロ酸ナトリウムにも4種類の結晶形の存在を確認したが，これらの結晶形について2水準の湿度条件下で厳密な吸湿実験を行ったところ，低湿度下では結晶形間で明確な吸湿

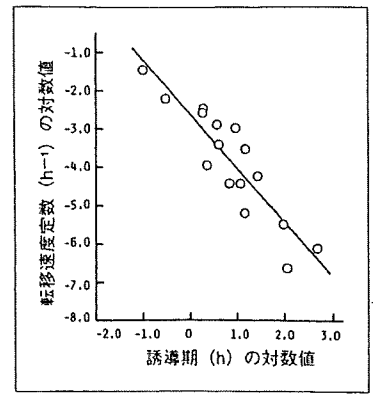

図3　フロセミドⅢ形からⅠ形への転移における誘導期と転移速度定数の関係

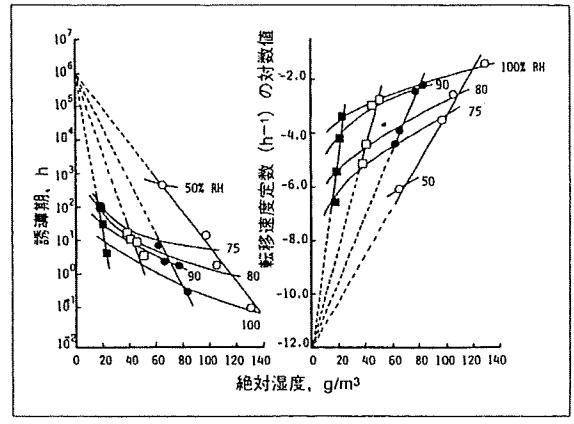

図4　フロセミドⅢ形結晶の転移における誘導期と転移速度定数に及ぼす絶対湿度と温度の影響

温度：○，60℃；●，50℃；□，40℃；■，25℃.

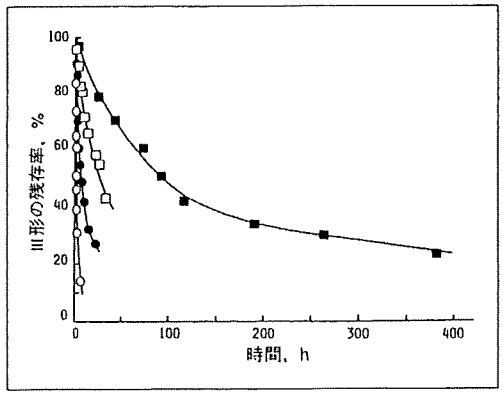

図2　フロセミドⅢ形からⅠ形への転移に及ぼす温度の影響(100% RH)

温度：○，60℃；●，50℃；□，40℃；■，25℃.

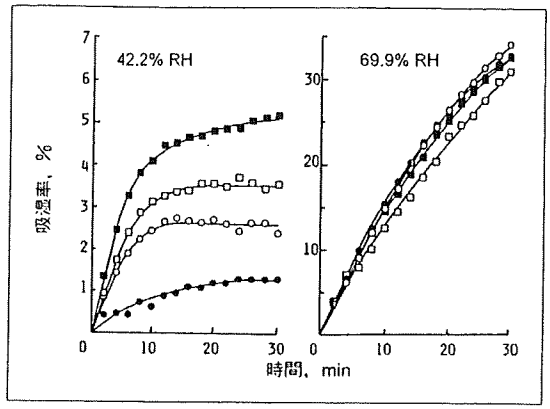

図5　25℃で保存されたバルプロ酸ナトリウム結晶多形の吸湿曲線

○, Ⅰ形：●, Ⅱ形：□, Ⅲ形：■, Ⅳ形.

特性の差異が認められたが，高湿度下ではこの差異は消滅し，いずれの結晶も潮解しながら急速に吸湿した(図5)．これらの結果から得られた臨界相対湿度は結晶間で異なり，34.5～44.6%となった．したがって，これらの医薬品の製剤工程では，臨界相対湿度を考慮した適切な湿度管理が必要である．

クロルプロパミドには5種類の結晶形(Ⅰ～Ⅴ形)が存在することが報告されている．筆者らは，これらの結晶形間の転移過程を種々の温度・湿度条件下で長期間にわたって詳細に追跡した．1例として図6に45℃における結果を示す．曲線のプロファイルから容易に推測されるように，結晶形によって転移機構が異なることが分かる．これらの結晶形のうち，Ⅰ，Ⅱ，Ⅲ形はいずれも安定形であるⅣ形へ直接に転移したのに対して，Ⅴ形は準安定形であるⅠ形を経由してⅣ形へ転移するという，逐次反応的な転移現象を示した．そこで，Ⅴ形の転移状態を3成分の残存率として三角図表にまとめると図7の結果が得られた．この逐次型転移系においては0% RHでは高温条件下(55℃)でも転移はⅠ形で停止しており，水分が存在しない乾燥条件下ではこのⅠ形は温度に対して十分に安定であるといえる．また，比較的緩和な保存条件(低温，低湿度)下では，Ⅴ形はⅠ→Ⅳ形ルートが律速過程となっているため，いったん完全にⅠ形へ転移した後，引き続きⅣ形へ転移した．これに対して，過酷条件下ではⅠ→Ⅳ系の転移速度定数が次第に増大するために，Ⅰ形の生成率が十分に増加しないうちにⅣ形へ転移した．そこで，反応速度式から得られた各結晶形の半減期を重回帰分析によって温度及び湿度を変数とする実験式として表わし，この式を用いて予測した半減期のシミュレーション・ダイアグラムを作成した(図8，半減

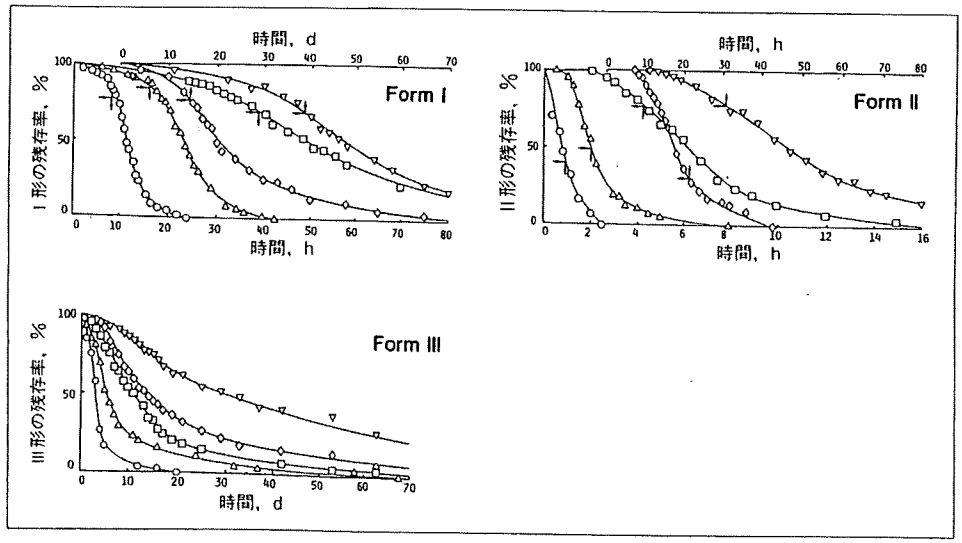

図6　種々の湿度下(45℃)におけるクロルプロパミドⅠ形，Ⅱ形，Ⅲ形からⅣ形結晶への転移の経時的変化

相対湿度：○, 100%：△, 85%：□, 70%：◇, 50%：▽, 0%.

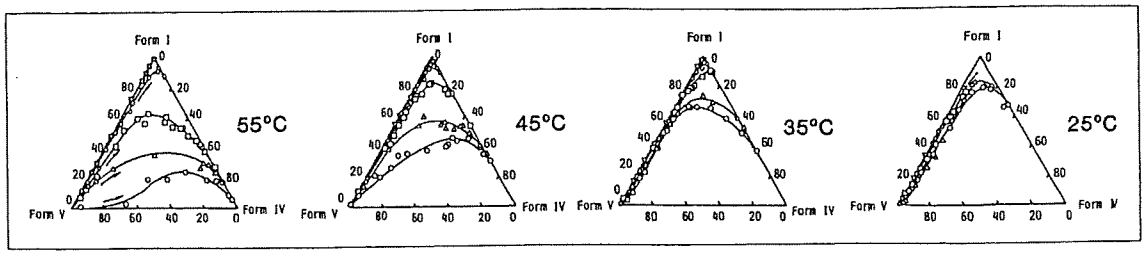

図7　クロルプロパミドのV形結晶のV→I→IV系転移における温度及び湿度の影響
相対湿度：○，100%；△，85%；□，70%；◇，50%；▽，30%；☆，0%．

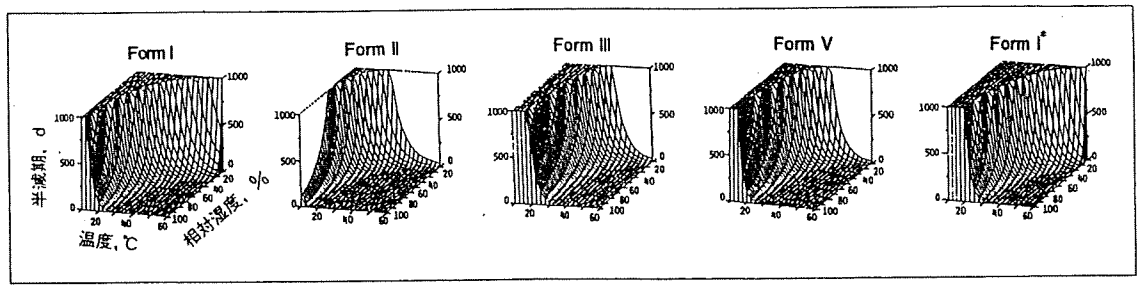

図8　種々の温度・湿度条件下におけるクロルプロパミドの4種類の準安定形の結晶転移における半減期のシミュレーション・ダイアグラム

期は1,000日で切断してある)．これらの立体図を鳥瞰すると，各結晶形の温度・湿度に対する安定性が一目瞭然で理解できる．すなわち，裾野の面積が広く，1,000日レベル面の面積が狭い結晶形(この場合，II形)ほど，温度・湿度のいずれに対しても不安定であるのに対して，逆にI形はこれらの因子のいずれに対しても比較的安定であり，III形とV形は湿度より温度に対する安定性に乏しいことが判明した．なお，この図において左端はI形結晶を用いて得られた結果であり，右端はV→I→IV系の転移過程から算出されたI形の結果であるが，両者のパターンは酷似していることが容易に理解できる．

6 まとめ

比較的低温条件下での速度論的安定性の評価に焦点を絞って展開された多形転移の研究例は，筆者らの報告以外にはほとんど見当たらない．固体医薬品の安定性研究において十分に信頼性の高い結果を得るためには，再現性が保証された調製法に基づいて得られた試料を用いて，綿密な実験計画のもとにデータを根気よく，かつ精細に集積していくことが必須である．このような観点から，たとえ地味な研究分野であっても結晶性医薬品の製剤の開発過程において不可欠な安定性研究に目を向けることは，大学のように時間的な制約を受けない研究機関に課せられた使命の1つであると考えている．

文　献

1) Chemburkar S. R. *et al*., *Org. Process Res. Dev*., 4, 413 (2000).
2) Bauer J. *et al*., *Pharm. Res*., 18, 859 (2001).
3) Grunenberg A. *et al*., *Int. J. Pharm*., 129, 147 (1996).
4) Matsuda Y. *et al*., *Int. J. Pharm*., 60, 11 (1990).
5) Pudipeddi M. *et al*., *J. Pharm. Sci*., 94, 929 (2005).
6) Matsuda Y. *et al*., *J. Pharm. Sci*., 73, 1453 (1984).
7) Otsuka M. *et al*., *Chem. Pharm. Bull*., 45, 894 (1998).
8) Otsuka M. *et al*., *Coll. Surf. B : Biointerfaces*, 17, 145 (2000).
9) Kato F. *et al*., *Int. J. Pharm*., 321, 18 (2006).
10) Matsuda Y. *et al*., *J. Pharm. Pharmacol*., 44, 627 (1992).
11) Matsuda Y. *et al*., *J. Pharm. Sci*., 73, 173 (1984).
12) De Villiers M. M. *et al*., *Int. J. Pharm*., 88, 275 (1992).
13) Kojima T. *et al*., *Int. J. Pharm*., in press.
14) Matsuda Y. *et al*., *J. Pharm. Pharmacol*., 46, 162 (1994).
15) Teraoka R. *et al*., *Int. J. Pharm*., 286, 1 (2004).
16) 松田芳久，寺岡麗子，*Pharm. Tech. Jpn*, 22, 1049 (2006).

Available online at www.sciencedirect.com
ScienceDirect
International Journal of Pharmaceutics 336 (2007) 346–351
INTERNATIONAL JOURNAL OF PHARMACEUTICS
www.elsevier.com/locate/ijpharm

Effect of spectroscopic properties on photostability of tamoxifen citrate polymorphs

Takashi Kojima [a,*], Satomi Onoue [c], Fumie Katoh [a], Reiko Teraoka [a], Yoshihisa Matsuda [a], Shuji Kitagawa [a], Mitsutomo Tsuhako [b]

[a] Department of Pharmaceutical Technology, Kobe Pharmaceutical University, Higashi-Nada, Kobe 658-8558, Japan
[b] Department of Functional Molecular Chemistry, Kobe Pharmaceutical University, Higashi-Nada, Kobe 658-8558, Japan
[c] Department of Analytical Chemistry, Faculty of Pharmaceutical Sciences, Toho University, Funabashi, Chiba 274-8510, Japan

Received 7 September 2006; received in revised form 27 October 2006; accepted 14 December 2006
Available online 27 December 2006

Abstract

The photostability of tamoxifen citrate polymorphs, forms A and B, was investigated by chromatographic and spectroscopic analyses including high-pressure liquid chromatography (HPLC), colorimetry and UV/vis solid-state absorption spectroscopy. On the basis of the results of photostability studies under irradiation by visible light and both UVA (320–400 nm) and a fraction of UVB (290–320 nm) light, form A was chemically unstable, whereas form B was stable against light irradiation. The surface color of pellets prepared with any of these crystal forms turned from white to brown; however, the extent of color change in cross-sections of form A pellet was deeper than that of form B pellet. The maximum peak of UV/vis solid-state absorption spectra of form A was observed at 337 nm within the UVA range and was in longer wavelength regions than form B, which exhibited the strong UV absorption mainly in UVB and UVC region. The results obtained suggested that the photodegradation followed by surface color change of form A crystal was caused by the selective absorption of photoenergy of UVA light irradiated by a xenon lamp.

Keywords: Pre-formulation; Solid-state stability; Photostability; Polymorphism; Crystal form; UV/vis spectroscopy

1. Introduction

During the process of drug development, stability has been identified as an essential element to assure the safety and efficacy of drug products because of the possibility of toxic degradants and loss of active ingredient (Yasueda et al., 2004). In particular, the solid-state stability of drug substances in the early stage of drug development would impact on the selection of the solid form, formulation and packaging (Aman and Thoma, 2002; Byrn et al., 2001; Huang and Tong, 2004; Matsuda and Mihara, 1978; Ragno et al., 2003; Waterman and Adami, 2005). The solid-state stability of crystalline drugs is generally classified into various categories, including physical and chemical stability. Physical stability represents the stability in crystalline form, in which the transformation of polymorphs and pseudopolymorphs would occur under some storage conditions relating to humidity and temperature. Chemical stability represents resistance against chemical reactions such as oxidization, dimerization and degradation. It is well known that the polymorphism of drug substances sometimes affects their physical and chemical stability (Gandhi et al., 2000; Matsuda and Tatsumi, 1990; Maurin et al., 2002; Otsuka et al., 1991, 1993), possibly due to differences in molecular arrangement.

Recently, the number of photosensitive drugs has noticeably increased, and articles dealing with the relationship between crystal forms and their photochemical stability have been reported (Akimoto et al., 1985; Glass et al., 2004; Nord et al., 1997; Teraoka et al., 2004). Pellets of three polymorphs of carbamazepine showed different photostability as detected by Fourier-transformed infrared reflection-absorption spectrometry and colorimetry (Matsuda et al., 1994). Pellets of four polymorphs and two pseudopolymorphs of furosemide also showed different photostability as detected by colorimetry and kinetic study of photodegradation was elucidated (De Villiers et al., 1992; Matsuda and Tatsumi, 1990). Thus, the photostability of polymorphs has been investigated to some extent, although

* Corresponding author. Tel.: +81 78 441 7531; fax: +81 78 441 7532.
E-mail address: tak_kojimajpn@yahoo.co.jp (T. Kojima).

0378-5173/$ – see front matter © 2006 Elsevier B.V. All rights reserved.
doi:10.1016/j.ijpharm.2006.12.025

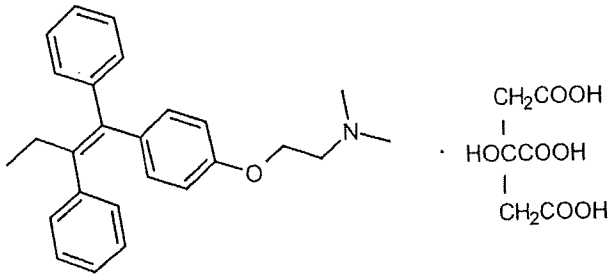

Fig. 1. Chemical structure of tamoxifen citrate.

the relationship between photostability and the physicochemical properties of crystals has not been fully elucidated.

In this paper, we focused on the photodegradation of tamoxifen citrate polymorphs caused by photochemical reaction, and investigated the relationship between photostability and UV/vis solid-state absorption spectra of the crystalline forms. Tamoxifen citrate (Fig. 1), clinically used as an antiestrogenic agent for the treatment of breast cancer (Pappas and Jordan, 2002), exhibits two crystalline forms, A and B (Goldberg and Becker, 1987). Tamoxifen has been also used as a model pharmaceutical compound for preformulation studies and many researches have been conducted (Bhatia et al., 2004; Brigger et al., 2001; Ho et al., 2004; Kojima et al., 2006; Shenoy and Amiji, 2005; Zeisig et al., 2004). Previously, tamoxifen was reported to be a photosensitive drug (Onoue and Tsuda, 2005; Salamoun et al., 1990; Wilson and Ruenitz, 1993), and the color change of tamoxifen citrate used for drug substances under sunlight irradiation was also described in the interview form issued by the manufacturer. We demonstrated solid-state photochemical evaluation of tamoxifen citrate polymorphs, forms A and B. A novel insight into the relationship between photostability and the spectroscopic properties of these crystals was also identified and discussed.

2. Material and methods

2.1. Preparation of polymorphs

Tamoxifen citrate was obtained from EGIS Pharmaceuticals (Budapest, Hungary). All solvents were purchased from Wako Pure Chemical Industries (Osaka, Japan). Tamoxifen citrate form A was a bulk powder purchased from EGIS Pharmaceuticals. Form B was obtained by crystallization from a saturated isopropyl alcoholic solution of the drug with stirring overnight at room temperature. Purity was assessed by RP-HPLC and crystalline forms were identified by powder X-ray diffractometry (PXRD), differential scanning calorimetry (DSC) and thermal gravimetric analysis (TGA).

2.2. High-pressure liquid chromatography (HPLC)

Tamoxifen was analyzed with an HPLC system (Model 510, Waters, Milford, MA, USA) and UV detector (Waters 486, Waters) operated at 205 nm. The packaged column was Inertsil ODS-3 (3 μm, 4.6 mm × 250 mm, GL Science, Tokyo, Japan) operated at 25 °C at a flow rate of 1.0 mL/min. The mobile phase consisted of acetonitrile:10 mM ammonium acetate buffer (80:20). After light irradiation, a powder sample in the glass vial was dissolved in methanol and subjected to an HPLC analysis for purity assessment.

2.3. Powder X-ray diffractometry

Powder X-ray diffraction patterns were recorded using a RINT Ultima (Rigaku, Tokyo, Japan) with Cu Kα radiation generated at 14 mA and 30 kV at room temperature. Data were collected from 2° to 40° (2θ) at a step size of 0.02° and scanning speed of 4° min^{-1}.

2.4. Thermal analysis

DSC was performed using a DSC-3100 system (Mac Science, Tokyo, Japan). The DSC thermogram was obtained from an aluminum open-pan system using a sample weight of ca. 5 mg and a heating rate of 10 °C/min under a nitrogen flow rate of 30 mL/min. TGA was performed using a TG/DTA 2000SA system (Bruker AXS, Madison, WI, USA). The TGA thermogram was obtained under the same conditions as those for DSC.

2.5. UV/vis solid-state spectroscopy

Diffuse reflectance UV/vis solid-state absorption spectra of tamoxifen citrate forms A and B were recorded on a UV-2450 system (Shimadzu, Kyoto, Japan) equipped with an integrating sphere unit (Shimadzu ISR-2200) at room temperature. A quartz cell was filled with sample powder and the spectra were acquired with 1.0 nm sampling pitch in the wavelength range from 190 to 700 nm.

2.6. Preparation of sample pellets

The sample powders were accurately weighed and compressed using an oil hydraulic press (WPM-2, Okada Seiko, Tokyo, Japan) equipped with flat-faced punches and cylindrical die (8 mm i.d.) set at a compression force of 10 kN for 30 s. After compression, crystalline forms of compressed pellets were assessed by PXRD. No polymorphic transformation occurred before and after compression for any of these crystalline forms.

2.7. Irradiation test

The powder and pellets of tamoxifen citrate forms A and B were placed in capped 10 mL glass vials (1.2 mm in thickness) and a six-well cell culture plate (Corning, NY, USA) covered with a glass plate (1.5 mm in thickness), respectively. Samples were stored in a light-irradiation tester (Light-Tron Xenon LTX-01, Nagano Science, Osaka, Japan) equipped with a 2 kW xenon lamp. The spectral irradiation energy of the lamp through an optical filter and infrared cutting filter (Nagano Science) ranged from 310 to 800 nm, with a maximum intensity of 470 nm.

Illuminance was set at 30,000 lx and the irradiation was carried at 25 °C. Illuminance (30,000 lx) was checked on a UVR-2 radiometer (Topcon, Tokyo, Japan) for each experimental procedure.

2.8. Colorimetric measurement

The surface color of the compressed sample pellet was measured with a chromameter (CCR-221, KONICA MINOLTA HOLDINGS, Tokyo, Japan) in the $L^*a^*b^*$ color system. Color difference (ΔE) between the intact and irradiated samples was calculated and all values were the averages of two determinations.

2.9. Statistics

Data for the depth of color changes on cross-section of pellets were expressed as the mean ± S.D. of at least 10 determinations for each experimental group, and were analyzed using Student's t-test. Differences were considered significant when $p < 0.01$.

3. Results

3.1. Solid-state photodegradation of form A and B crystals

The photostability test was performed with powder of forms A and B, for which crystalline forms were evaluated by PXRD (Fig. 2), DSC and TGA according to the data reported previously (Goldberg and Becker, 1987). HPLC chromatograms of intact samples indicated that the amount of impurity was extremely small and negligible. The powder in capped 10 mL glass vials was stored under light irradiation by a xenon lamp equipped with a cutting filter ranging from 310 to 800 nm. Polymorphic changes of crystalline forms after irradiation were assessed by PXRD, and no transformation was detected. After chronic light irradiation, each sample was subjected to HPLC analysis, and the purity was assessed and compared (Fig. 3). Several unidentified peaks, eluted within 3–5 min, were detected on HPLC chromatograms after irradiation to form A sample, suggesting that the photodegradation was induced. Without light irradiation, both forms A and B were stable at least during the period tested, because no significant peaks attributable to photoproducts were detected. Exposure of form A to xenon lamp for 30 days resulted in significant decrease of purity as low as 87% (Table 1). On the other hand, form B was quite photostable and the amount of tamoxifen remained 99% even after 30-day exaggerated irradiation. These results suggested that form A was photosensitive, whereas form B was quite resistant to photo-irradiation.

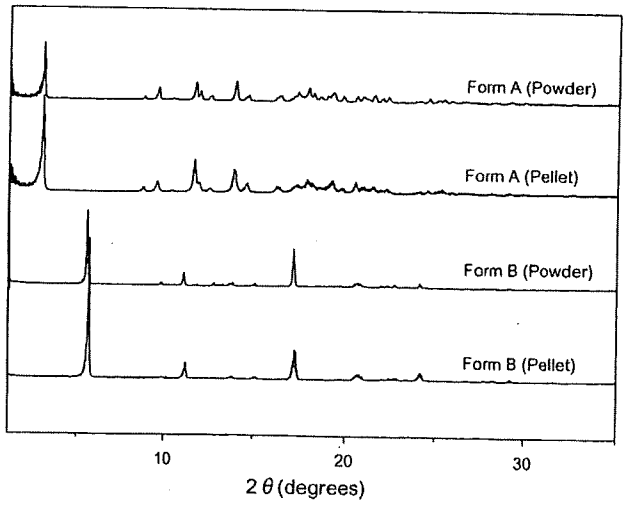

Fig. 2. PXRD patterns of forms A and B for irradiation tests.

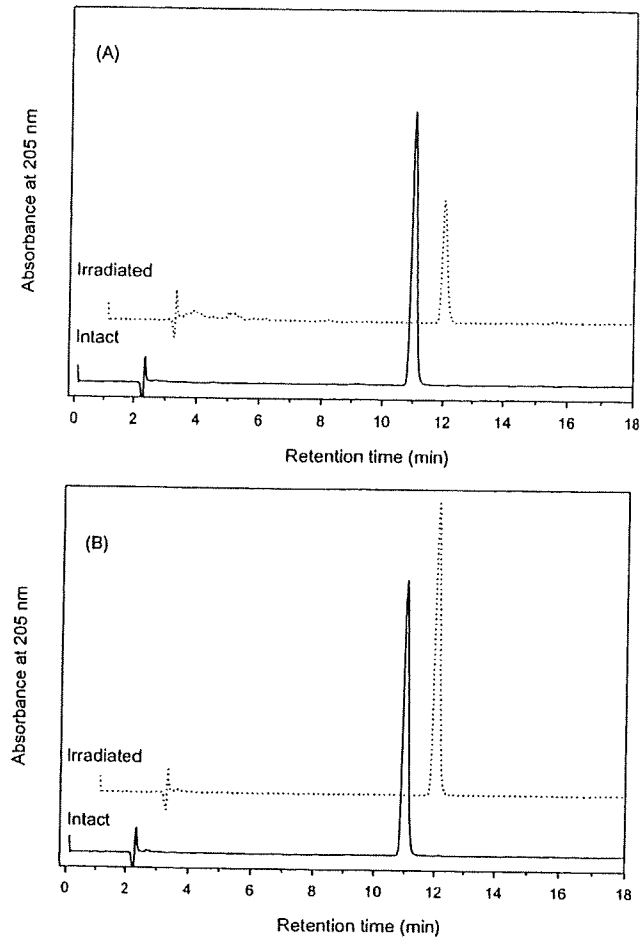

Fig. 3. HPLC chromatograms of forms A (A) and B (B) before irradiation (intact) and after 30-day irradiation (irradiated). Solid line (—), intact sample; dotted line (···), irradiated sample.

Table 1
Photodegradation of tamoxifen citrate forms A and B

Forms	Storage condition	Purity (percentage of total area)			
		Initial	10 days	20 days	30 days
Form A	Non-irradiated	100	99	99	99
	Photo-irradiated	–	94	92	87
Form B	Non-irradiated	100	99	99	100
	Photo-irradiated	–	99	99	100

Each compound was exposed to xenon lamp at the illuminance of 30,000 lx for the indicated periods, then subjected to an HPLC analysis.

Table 2
Color changes of pellets of tamoxifen citrate forms A and B before and after irradiation

Forms	Exposure period	L^*	a^*	b^*	ΔE
Form A	Initial	95.7	−0.3	−3.4	–
	5 days	88.5	−1.8	31.6	35.8
	10 days	85.4	−0.1	38.1	42.8
	20 days	83.2	2.1	43.5	48.6
	30 days	79.3	5.3	48.2	54.5
Form B	Initial	97.4	−0.1	−1.9	–
	5 days	94.5	−2.8	18.3	20.5
	10 days	93.0	−2.2	24.1	26.4
	20 days	90.1	−0.9	30.9	33.6
	30 days	90.9	−0.6	31.0	33.6

The a^* scale for green-red, the b^* scale for yellow-blue, L^* scale for black-white and ΔE for color difference.

3.2. Discoloration of form A and B pellets after light irradiation

The color changes of forms A and B were assessed with pellets prepared from these forms. Polymorphic changes of these crystalline forms after irradiation were assessed by PXRD, and the data obtained clearly showed no polymorphic transformation even after long-term light irradiation. Intact and irradiated samples were subjected to colorimetric measurement to compare the surface color changes of pellets before and after irradiation. The surface color of pellets prepared from form A significantly turned from light white to dark brown upon exposure to light. On the other hand, the surface color of form B pellets gradually turned from light white to light brown. Color changes before and after irradiation were evaluated by two chromaticness coordinates (a^* scale for green-red and b^* scale for yellow-blue), the illuminance coordinate (L^* scale for black-white) and color difference (ΔE) before and after irradiation (Table 2). Although the a^* scale of both crystal forms was almost invariable, the L^* and b^* scales remarkably decreased (turned to black) and increased (turned to yellow) after the elapsed irradiation time, respectively. Thus, changes in the $L^*a^*b^*$ system suggested that forms A and B turned to brown. The ΔE values of forms A and B after 30-day irradiation increased up to 54.5 and 33.6, respectively. The ΔE value of form A was much greater than that of form B at any irradiation time, suggesting that form A discolored more sensitively as compared to form B.

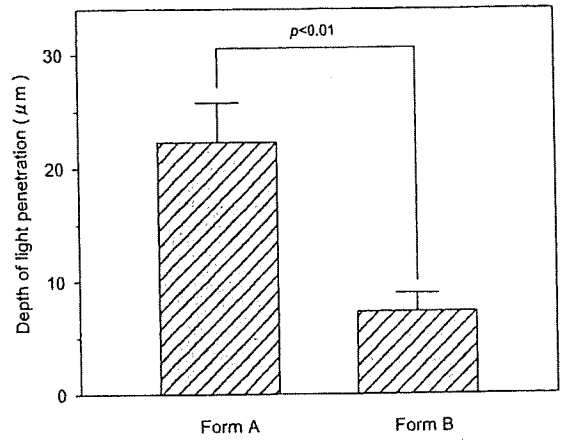

Fig. 5. Depth of light penetration measured as color changes in the cross-sections of forms A and B pellets. Each column represents the mean ± S.D. of at least 10 determinations for each experimental group. Significantly different between forms A and B; $p < 0.01$.

The thickness of the discoloration layer was assessed in cross-sections of form A and B pellets. After colorimetric measurement of the pellet surface, the pellets were cut with a razor for microscopic observation of cross-sections. The similar void ratio of these pellets, obtained from the apparent densities of pellets and particle densities of forms A and B, should result in a depth of color change corresponding to light penetration. The depth of color changes on cross-sections of pellets, as a measure for light penetration into the pellets, was measured and the results are shown in Fig. 4. The color of cross-sections of pellets prepared from forms A and B turned from light white to dark brown and light brown upon exposure to UV light, respectively. The depth of the discolored layer in cross-sections of form A and B pellets after 30-day irradiation was 22.3 ± 3.5 and 7.3 ± 1.6 μm, respectively ($p < 0.01$) (Fig. 5). These results suggested that light penetration was far deeper in form A pellets than form B pellets, irrespective of the same porosity.

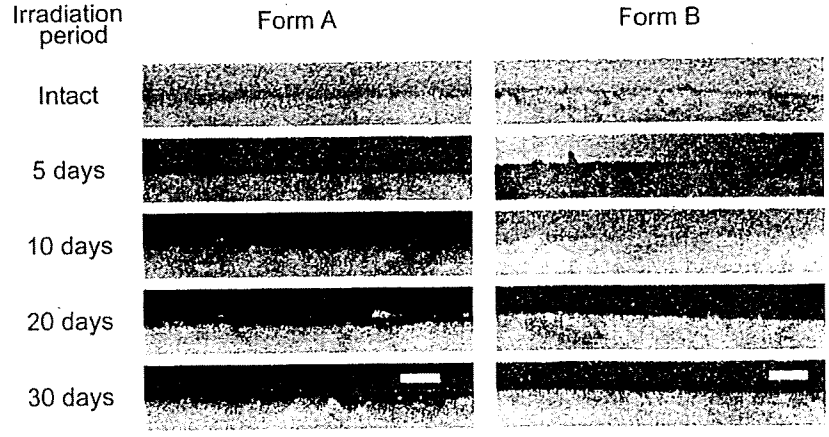

Fig. 4. Photomicrographs of cross-sections of form A and B pellets under UV light irradiation for 5, 10, 20 and 30 days. Scale bar represented 100 μm.

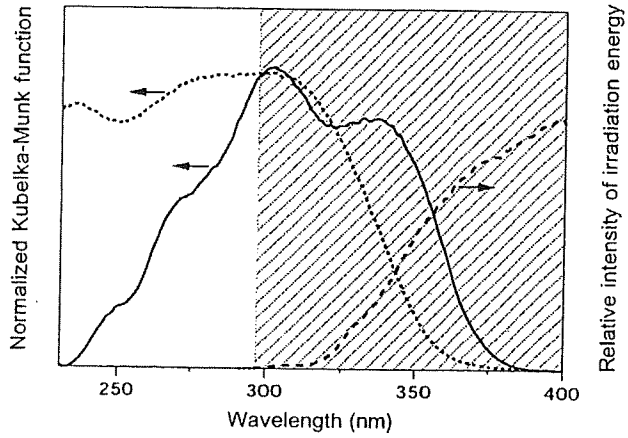

Fig. 6. Ultraviolet absorption spectra of forms A and B. Solid line (—), form A; dotted line (···), form B; broken line (- - -), xenon lamp. Hatched region; irradiation wavelength range by xenon lamp.

3.3. Spectroscopic properties of form A and B crystals

The photostability of solid pharmaceutical substances depends on many factors, i.e., surface area and photochemical properties of the sample, and the irradiation conditions such as spectral irradiation energy and even type of the light source. Although most of these parameters can be controlled, the photochemical properties of samples are uncontrollable, because these are the intrinsic properties depending on the molecular structure. In this study, the solid-state absorption spectra in the UV/vis region were investigated in order to elucidate the relationship between photostability and photochemical properties. Diffuse reflectance UV/vis solid-state absorption spectra of forms A and B were recorded on a spectrophotometer equipped with an integrating sphere unit at room temperature, and compared with the spectral irradiation intensity pattern of a xenon lamp to assess the absorbability of photoenergy by these crystals (Fig. 6). In this figure, the maximum values of Kubelka–Munk function for forms A and B are modified so as to be equal to easily enable qualitative comparison of difference in spectra of these forms and spectral irradiation pattern simulating sunlight. The irradiation light passing through a filter (310–800 nm) was composed of visible light (>400 nm), UVA (320–400 nm) and a fraction of UVB (290–320 nm). Form B exhibited the strong UV absorption mainly in the UVB and UVC region. In contrast, the maximum peak absorption of form A was clearly observed at 337 nm in the UVA range and was at a longer wavelength (bathochromic shift) than form B. On the basis of the photostability data, these results suggested that form A would absorb much more photoenergy than form B, resulting in easier photoexcition and the formation of photoproducts upon exposure to UVA light.

4. Discussion

We have demonstrated for the first time that the difference in photostability between tamoxifen citrate polymorphs, forms A and B is associated with their spectroscopic properties, solid-state UV/vis absorption spectra, due to different molecular arrangements in the crystal lattice. According to the data shown in Tables 1 and 2, we revealed that form A was unstable, whereas form B was stable under photo-irradiation. The results of the UV/vis solid-state absorption spectra of these crystal forms showed that the maximum absorption peak was observed at 337 nm in the UVA range for form A and was at a longer wavelength than form B which exhibited the strong UV absorption mainly in the UVB and UVC region. The wavelength of light radiated from a xenon lamp ranged from 310 to 800 nm, composed of visible light, UVA (320–400 nm) and a fraction of UVB (290–320 nm). Taking these results into account, the photoinstability and depth of color changes of form were caused by the selective absorption of photoenergy of UVA light radiated by a xenon lamp.

Under light irradiation, drug molecules absorb photon energy and molecules are excited in the singlet state. The excitation energy in the singlet state is generally dissipated as fluorescence, heat or exhausted in photochemical reactions caused by reactive oxygen spices such as singlet oxgen ($^1O_2$) and superoxide (O_2^-) generated from photo-irradiated substances (Onoue and Tsuda, 2005). Different crystal structures due to polymorphism should exhibit different energy states. Recently, the differences of solid-state fluorescence as a photophyisical property among polymorphs were discussed and elucidated (Brittain et al., 2005; Kaczmarek and Kaczmarski, 1996). Apart from these researches, we investigated the solid-state photoreaction, which possibly affects the photostability of polymorphs. However, to the best of our knowledge, the relationship between photostability and the photophysical properties of crystal forms was not elucidated.

With respect to UV/vis spectroscopy in solution, the maximum absorption spectra band shifted to longer or shorter wavelengths depending on the condition, such as dissolving solvents, which was called solvent shift, caused by solvent–solute interaction due to the dipole moment transformation of chromophore during excitation (Naseem et al., 2004; Verdasco and Martín, 1995). Recently, attention has also been drawn to the solid-state absorption spectra band shift (Aman and Thoma, 2003; Mizuguchi et al., 1995; Stockton et al., 1998). In the solid state, the absorption spectra band shift is caused by intra/intermolecular interaction, which may depend on its crystal packing surrounded by chromophores during excitation. Thus, this polymorphism could be dominant for the absorption spectra in the solid state.

Tamoxifen was known as a photosensitive drug and generate superoxide after UVA/UVB irradiation (Onoue and Tsuda, 2005). It was also reported that tamoxifen was photochemically converted into phenanthrene derivative under UV irradiation in the solution state (Salamoun et al., 1990). We have conducted the solid-state photostability studies on tamoxifen citrate and demonstrated that form A was photosensitive and the different photosensitivity among polymorphs was caused by specific UV/vis solid-state absorption spectra, probably depending on crystal packing surrounded by chromophores during excitation. In drug development, photosensitivity impacts on the formulation, manufacturing process, packaging and storage conditions. Information about the photosensitivity of solid drug substances

could make it possible to reduce development costs. Based on the results of this study, form B could be said to be a suitable form for reasonable development from the viewpoint of medical economics.

In conclusion, we have provided a novel insight into the photosensitivity of tamoxifen citrate polymorphs. We also demonstrated that solid-state absorption spectra could be used as a useful method for the photophysical characterization of polymorphs. In the development of photosensitive drug substances, solid-state absorption spectra may provide key information about photosensitivity.

References

Akimoto, K., Inoue, K., Sugimoto, I., 1985. Photo-stability of several crystal forms of cianidanol. Chem. Pharm. Bull. (Tokyo) 33, 4050–4053.

Aman, W., Thoma, K., 2002. The influence of formulation and manufacturing process on the photostability of tablets. Int. J. Pharm. 243, 33–41.

Aman, W., Thoma, K., 2003. Particular features of photolabile substances in tables. Pharmazie 58, 645–650.

Bhatia, A., Kumar, R., Katare, O.P., 2004. Tamoxifen in topical liposomes: development, characterization and in vitro evaluation. J. Pharm. Pharm. Sci. 7, 252–259.

Brigger, I., Chaminade, P., Marsaud, V., Appel, M., Besnard, M., Gurny, R., Renoir, M., Couvreur, P., 2001. Tamoxifen encapsulation within polyethylene glycol-coated nanospheres. A new antiestrogen formulation. Int. J. Pharm. 214, 37–42.

Brittain, H.G., Elder, B.J., Isbester, P.K., Salerno, A.H., 2005. Solid-state fluorescence studies of some polymorphs of diflunisal. Pharm. Res. 22, 999–1006.

Byrn, S.R., Xu, W., Newman, A.W., 2001. Chemical reactivity in solid-state pharmaceuticals: formulation implications. Adv. Drug Deliv. Rev. 48, 115–136.

De Villiers, M.M., van der Watt, J.G., Lötter, A.P., 1992. Kinetic study of the solid-state photolytic degradation of two polymorphic forms of furosemide. Int. J. Pharm. 88, 275–283.

Gandhi, R.B., Bogardus, J.B., Bugay, D.E., Perrone, R.K., Kaplan, M.A., 2000. Pharmaceutical relationships of three solid state forms of stavudine. Int. J. Pharm. 201, 221–237.

Glass, B.D., Novák, C., Brown, M.E., 2004. The thermal and photostability of solid pharmaceuticals. J. Therm. Anal. Calorim. 77, 1013–1036.

Goldberg, I., Becker, Y., 1987. Polymorphs of tamoxifen citrate: detailed structural characterization of the stable form. J. Pharm. Sci. 76, 259–264.

Ho, S., Calder, R.J., Thomas, C.P., Heard, C.M., 2004. In vitro transcutaneous delivery of tamoxifen and gamma-linolenic acid from borage oil containing ethanol and 1,8-cineole. J. Pharm. Pharmacol. 56, 1357–1364.

Huang, L.F., Tong, W.Q., 2004. Impact of solid state properties on developability assessment of drug candidates. Adv. Drug Deliv. Rev. 56, 321–334.

Kaczmarek, F., Kaczmarski, M., 1996. Raman and fluorescence spectra of erbium pentaphosphate polymorphs. J. Raman Spectrosc. 27, 645–648.

Kojima, T., Onoue, S., Murase, N., Katoh, F., Mano, T., Matsuda, Y., 2006. Crystalline form information from multi-well plate salt screening by use of Raman microscopy. Pharm. Res. 23, 806–812.

Matsuda, Y., Mihara, M., 1978. Coloration and photolytic degradation of some sulfonamide tablets under exaggerated and ordinary ultraviolet irradiation. Chem. Pharm. Bull. (Tokyo) 26, 2649–2656.

Matsuda, Y., Tatsumi, E., 1990. Physicochemical characterization of furosemide modifications. Int. J. Pharm. 60, 11–26.

Matsuda, Y., Akazawa, R., Teraoka, R., Otsuka, M., 1994. Pharmaceutical evaluation of carbamazepine modifications: comparative study for photostability of carbamazepine polymorphs by using Fourier-transformed reflection-absorption infrared spectroscopy and colorimetric measurement. J. Pharm. Pharmacol. 46, 162–167.

Maurin, M.B., Vickery, R.D., Rabel, S.R., Rowe, S.M., Everlof, J.G., Nemeth, G.A., Campbell, G.C., Foris, C.M., 2002. Polymorphism of roxifiban. J. Pharm. Sci. 91, 2599–2604.

Mizuguchi, J., Rihs, G., Karfunkel, H.R., 1995. Solid-state spectra of titanylphthalocyanine as viewed from molecular distortion. J. Phys. Chem. 99, 16217–16227.

Naseem, B., Sabri, A., Hasan, A., Shah, S.S., 2004. Interaction of flavonoids within organized molecular assemblies of anionic surfactant. Colloids Surf. B Biointerfaces 35, 7–13.

Nord, K., Andersen, H., Tønnesen, H.H., 1997. Photoreactivity of biologically active compounds. XII. Photostability of polymorphic modifications of chloroquine diphosphate. Drug Stab. 1, 243–248.

Onoue, S., Tsuda, Y., 2005. Analytical studies on the prediction of photosensitive/phototoxic potential of pharmaceutical substances. Pharm. Res. 23, 156–164.

Otsuka, M., Teraoka, R., Matsuda, Y., 1991. Physicochemical stability of nitrofurantoin anhydrate and monohydrate under various temperature and humidity conditions. Pharm. Res. 8, 1066–1068.

Otsuka, M., Onoe, M., Matsuda, Y., 1993. Physicochemical stability of phenobarbital polymorphs at various levels of humidity and temperature. Pharm. Res. 10, 577–582.

Pappas, S.G., Jordan, V.C., 2002. Chemoprevention of breast cancer: current and future prospects. Cancer Metast. Rev. 21, 311–321.

Ragno, G., Cione, E., Garofalo, A., Genchi, G., Ioele, G., Risoli, A., Spagnoletta, A., 2003. Design and monitoring of photostability systems for amlodipine dosage forms. Int. J. Pharm. 265, 125–132.

Salamoun, J., Macka, M., Nechvatal, M., Matousek, M., Knesel, L., 1990. Identification of products formed during UV irradiation of tamoxifen and their use for fluorescence detection in high-performance liquid chromatography. J. Chromatogr. 514, 179–187.

Shenoy, D.B., Amiji, M.M., 2005. Poly(ethylene oxide)-modified poly(epsilon-caprolactone) nanoparticles for targeted delivery of tamoxifen in breast cancer. Int. J. Pharm. 293, 261–270.

Stockton, G.W., Godfrey, R., Hitchcock, P., Mendelsohn, R., Mowery, P.C., Rajan, S., Walker, A.F., 1998. Crystal polymorphism in pendimethalin herbicide is driven by electronic delocalization and changes in intramolecular hydrogen bonding. A crystallographic, spectroscopic and computational study. J. Chem. Soc. Perkin Trans. 2, 2061–2071.

Teraoka, R., Otsuka, M., Matsuda, Y., 2004. Evaluation of photostability of solid-state nicardipine hydrochloride polymorphs by using Fourier-transformed reflection-absorption infrared spectroscopy—effect of grinding on the photostability of crystal form. Int. J. Pharm. 286, 1–8.

Verdasco, G., Martín, M.A., del Castillo, B., López-Alvarado, P., Menéndez, J.C., 1995. Solvent effects on the fluorescent emission of some new benzimidazole derivatives. Anal. Chim. Acta 303, 73–78.

Waterman, K.C., Adami, R.C., 2005. Accelerated aging: prediction of chemical stability of pharmaceuticals. Int. J. Pharm. 293, 101–125.

Wilson, S., Ruenitz, P.C., 1993. Structural characterization and biological effects of photocyclized products of tamoxifen irradiation. J. Pharm. Sci. 82, 571–574.

Yasueda, S., Higashiyama, M., Shirasaki, Y., Inada, K., Ohtori, A., 2004. An HPLC method to evaluate purity of a steroidal drug, loteprednol etabonate. J. Pharm. Biomed. Anal. 36, 309–316.

Zeisig, R., Ruckerl, D., Fichtner, I., 2004. Reduction of tamoxifen resistance in human breast carcinomas by tamoxifen-containing liposomes in vivo. Anticancer Drugs 15, 707–714.

Physicochemical Characterization of Tamoxifen Citrate Pseudopolymorphs, Methanolate and Ethanolate

Takashi KOJIMA,*[,a] Fumie KATO,[a] Reiko TERAOKA,[a] Yoshihisa MATSUDA,[a] Shuji KITAGAWA,[a] and Mitsutomo TSUHAKO[b]

[a] *Department of Pharmaceutical Technology, Kobe Pharmaceutical University; and* [b] *Department of Functional Molecular Chemistry, Kobe Pharmaceutical University; Higashi-Nada, Kobe 658–8558, Japan.*

Received October 4, 2006; accepted December 15, 2006; published online December 20, 2006

Two novel pseudopolymorphs, methanolate and ethanolate of tamoxifen [(*Z*)-2-[4-(1,2-diphenyl-1-butenyl)-phenoxy]-*N*,*N*-dimethylethylamine]citrate, were prepared in addition to forms A and B reported previously. Their crystalline forms were identified and characterized by powder and single crystal X-ray diffractometry, differential scanning calorimetry, thermogravimetric analysis, hot-stage microscopy, scanning electron microscopy and diffuse reflectance infrared Fourier-transform spectroscopy, and their physicochemical stability was also evaluated. The results of single crystal X-ray analysis and thermogravimetric analysis of methanolate and ethanolate suggested that the stoichiometry of tamoxifen citrate : methanol and tamoxifen citrate : ethanol could be composed of a 1 : 1 molecular ratio for both solvates. The results of physicochemical stability evaluations at 75 and 97% RH at 40 and 60 °C indicated that the metastable form A was quite stable for at least 2 months even under severe storage conditions, whereas methanolate immediately transformed to a crystalline mixture of forms A and B, and subsequently changed to the stable form B.

Key words tamoxifen; pseudopolymorph; physicochemical characterization; physicochemical stability

During the development process of solid drugs, the most desirable crystal form should be appropriately selected based on the information of physicochemical properties including polymorphism, their salt[1,2] and co-crystal formation[3] of drug candidates, because physicochemical properties can affect efficacy, safety,[4—6] stability,[7,8] manufacturing process[9,10] and quality control.[11] Recently, understanding the polymorphism has been positioned as an important research, since polymorphs and pseudopolymorphs show different physicochemical properties[7,8,12—18] including solubility.[6] Generally, a stable polymorph shows low solubility and high stability, and metastable polymorphs exhibit higher solubility and lower stability. From the viewpoint of the manufacturing process, information about organic solvates is also valuable for the selection of a crystallization solvent. Appropriate selection of the crystalline form from polymorphs and pseudopolymorphs should be conducted in order to achieve the purposes of development; this contributes to the improvement of stability, bioavailability and manufacturability.

Tamoxifen, (*Z*)-2-[4-(1,2-diphenyl-1-butenyl)phenoxy]-*N*,*N*-dimethylethylamine, is one of the selective estrogen receptor modulators and tamoxifen citrate is widely used as a drug for the treatment of breast cancer. Tamoxifen has also been used as a model pharmaceutical compound for preformulation studies and several researches have been conducted.[2,19—23] As for tamoxifen citrate (Fig. 1), two polymorphs, forms A and B, were identified.[24] Previously, we have investigated the photostability of forms A and B, and discussed the difference in photostability from the viewpoint of solid-state UV/Vis absorption spectroscopy.[25] Even though tamoxifen citrate is widely used throughout the world, detailed characterization of its polymorphs and pseudopolymorphs has not been reported to the best of our knowledge.

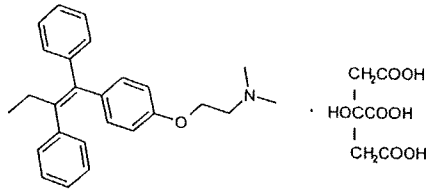

Fig. 1. Chemical Structure of Tamoxifen Citrate

In this study, we prepared two novel pseudopolymorphs, methanolate and ethanolate, in addition to forms A and B reported previously. Their crystal forms were identified and characterized by powder and single crystal X-ray diffractometry, differential scanning calorimetry (DSC), thermogravimetric analysis (TGA), hot-stage microscopy, scanning electron microscopy (SEM) and diffuse reflectance infrared Fourier-transform spectroscopy (DRIFTS), and their physicochemical stability was also evaluated.

Experimental

Preparation of Modifications Tamoxifen citrate was obtained from EGIS Pharmaceuticals (Budapest, Hungary). All solvents were purchased from Wako Pure Chemical Industries (Osaka, Japan). Form A was bulk powder purchased from EGIS Pharmaceuticals. A small amount of form A for SEM observation was obtained by recrystallizing from saturated acetonitrile solution of the drug by seeding a small amount of bulk powder. Form B was obtained by recrystallizing from saturated isopropyl alcoholic solution of the drug with stirring overnight at room temperature. Form B was then filtrated and dried *in vacuo* at room temperature. Methanolate and ethanolate were obtained by recrystallizing from saturated methanolic and ethanolic solutions of the drug with stirring overnight at room temperature, respectively. Methanolate and ethanolate were then filtrated and dried in a nitrogen atmosphere.

Scanning Electron Microscopy Scanning electron micrographs were taken on a scanning electron microscope (JSM-5200LV, JEOL, Tokyo, Japan) at magnifications of 200—1000×. All powder samples were coated with thin gold film in an ion-sputter coater (JFC-1100, JEOL).

Powder and Single Crystal X-Ray Diffractometries Powder X-ray diffraction patterns were recorded using a RINT Ultima (Rigaku, Tokyo, Japan) with Cu$K\alpha$ radiation generated at 30 kV and 14 mA at room temperature. Data were collected within diffraction angles from 2—40° (2θ) at a step size of 0.02° and a scanning speed of 4°/min.

Single crystal X-ray diffraction data were recorded on a SMART APEX II CCD X-ray diffractometer (Bruker AXS, Madison, WI, U.S.A.) with a Mo anode source at 90 K. The crystal structures were solved and refined using SHELXTL software.

* To whom correspondence should be addressed. e-mail: tak_kojimajpn@yahoo.co.jp

Thermal Analysis DSC was performed using a DSC 6200 system (Seiko Instruments, Chiba, Japan). A DSC thermogram was obtained in an aluminum open-pan system using a sample weight of *ca.* 3 mg and a heating rate of 5 °C/min under a nitrogen flow. TGA was performed using a TG/DTA 6200 system (Seiko Instruments). A TGA thermogram was obtained under the same conditions as those for DSC.

Thermal changes of crystal morphology were observed on a hot-stage microscope (LK-FDCS, Linkam Scientific Instruments, Surrey, U.K.) with a heating rate of 10 °C/min in a nitrogen flow.

Diffuse Reflectance Infrared Fourier-Transform Spectroscopy The FT-IR spectra of tamoxifen citrate polymorphs were recorded on a Spectrum One, Fourier-transform IR spectrometer (Perkin-Elmer, Wellesley, MA, U.S.A.) with diffuse reflectance after dispersion with KBr at room temperature. The samples were diluted with KBr to give 5% (w/w) mixture. A total of 64 scans was collected on each sample with 8 cm^{-1} resolution. The spectra obtained were transformed to the Kubelka–Munk function unit for standardization.

Physicochemical Stability The physicochemical stability of forms A and B, methanolate, and ethanolate was evaluated by storing each *ca.* 500 mg of the sample at 75 and 97% RH at 40 and 60 °C in desiccators. Samples were removed after 3, 7, 14, 28 and 56 d and the crystal forms were evaluated by PXRD, DSC and TGA. Storage conditions were adjusted with saturated aqueous solutions of NaCl (75% RH) and K_2SO_4 (97% RH).

Results and Discussion

Crystal Morphology Morphological differences among crystal forms were observed using scanning electron microscopy (SEM) (Fig. 2). Form A crystals had a spindly needle shape, whereas form B crystals had a column shape. The appearances of methanolate and ethanolate crystals were similar and they were composed of needle-like agglomerates and were far smaller than form B crystals.

Powder X-Ray and Single Crystal Diffraction Analyses Powder X-ray diffraction (PXRD) patterns of crystal forms are shown in Fig. 3. The characteristic diffraction peaks of form A were observed at 2.9, 9.4, 11.6 and 13.8° (2θ), while those of form B were observed at 5.6, 12.7, 17.1 and 24.0° (2θ). Thus, significant differences between forms A and B were observed and PXRD patterns agreed well with the data reported previously.[24] The characteristic X-ray diffraction peaks of methanolate were observed at 4.9, 9.7, 14.2 and 21.6° (2θ), while those of ethanolate were observed at 4.7, 9.5, 13.9 and 21.4° (2θ), showing slight shifts to lower diffraction angles. Thus, methanolate and ethanolate showed quite similar PXRD patterns with 0.2°-shift. The crystal structures of form B, methanolate and ethanolate were analyzed by single crystal X-ray diffractometry. The results indicated that form B crystals (size=0.11×0.08×0.03 mm) were monoclinic (a=15.881(3), b=22.048(5), c=8.4701(18) Å, β=95.427(3)°), space group $P2_1/c$ (Z=4, density=1.268 g/cm^3, R_1=0.0537), which coincided with the data reported already.[24] Methanolate (size=0.14×0.03×0.01 mm) and ethanolalte (size=0.17×0.03×0.01 mm) were also monoclinic (a=10.612(5), b=16.479(8), c=36.35(2) Å, β=94.164(12)°) and space group $P2_1/n$ (Z=4, density=1.246 g/cm^3, R_1=0.1008), and monoclinic (a=10.639(2), b=16.512(3), c=36.707(8) Å, β=93.108(6)°) and space group $P2_1/n$ (Z=4, density=1.258 g/cm^3, R_1=0.0981), respectively. The results of single crystal analysis of methanolate and ethanolate also clearly indicated that arrangements of tamoxifen and citric acid molecules in the crystal were similar and the stoichiometry of tamoxifen citrate : methanol and tamoxifen citrate : ethanol was confirmed to be a 1 : 1 molecular ratio for any solvate (Fig. 4a). Hydrogen bonds between alcohol molecule and terminal carboxylic function of citric acid molecule were observed and resulted in differences of intermolecular interaction between adjacent citrate species compared with form B crystals in which a 9-membered circle hydrogen bond was formed (Fig. 4b).[24] However, a single crystal of form A, of sufficient size for sin-

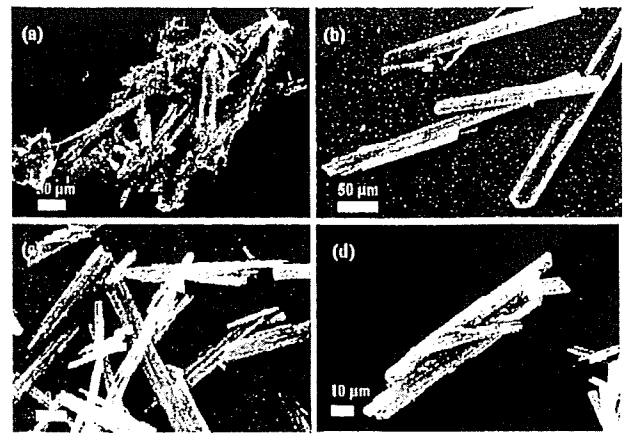

Fig. 2. Scanning Electron Photographs of Tamoxifen Citrate Modifications

(a) Form A; (b) form B; (c) methanolate; (d) ethanolate.

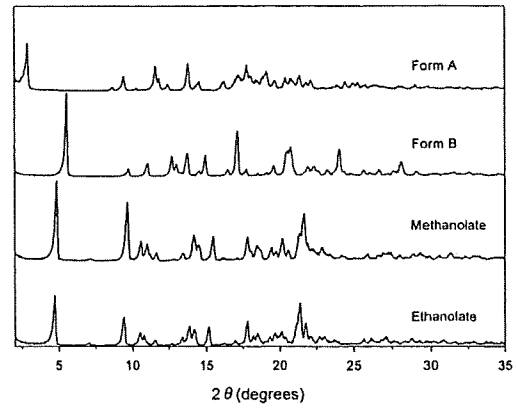

Fig. 3. PXRD Patterns of Forms A and B, Methanolate and Ethanolate

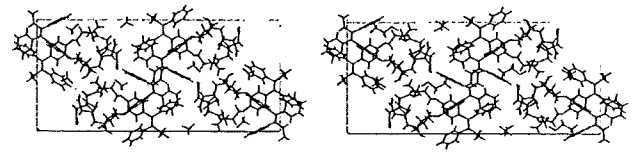

Fig. 4a. Crystal Structures of Methanolate and Ethanolate

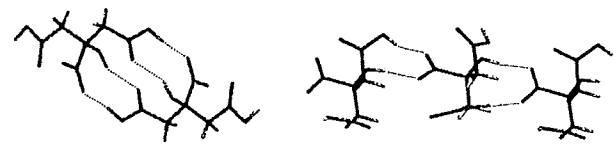

Fig. 4b. Cyclic Pairs of Hydrogen Bonding of Citrate Species in Form B and Methanolate Crystals

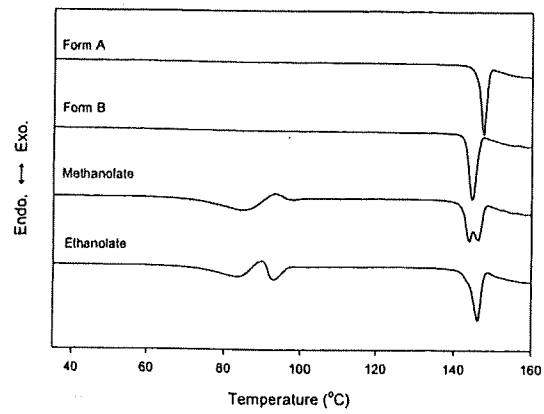

Fig. 5. DSC Thermograms of Forms A and B, Methanolate and Ethanolate

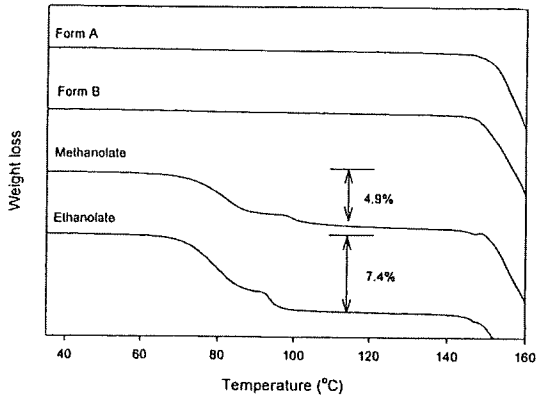

Fig. 6. TGA Thermograms of Forms A and B, Methanolate and Ethanolate

gle crystal X-ray analysis, could not be obtained, even though crystallization was extensively attempted under various conditions.

Thermal Properties DSC curves of forms A and B showed melting endothermic peaks at 147.5 and 144.8 °C, respectively (Fig. 5). The heat of fusion (ΔH_f) of forms A and B was 59.7 and 63.7 kJ/mol, respectively, thus indicating that these forms have quite similar thermal properties. The DSC curve of methanolate seemed to show an endothermic peak at 85.7 and 98.1 °C, an exothermic peak at 94.1 °C, then two endothermic peaks at 144.2 and 146.5 °C, which corresponded with the melting points of forms B and A, respectively. The DSC curve of ethanolate also seemed to show two endothermic peaks at 84.1 and 94.0 °C, an exothermic peak at 90.4 °C, then two endothermic peaks at 143.5 and 146.3 °C, which corresponded with the melting points of forms B and A, respectively. The results of TGA thermograms of methanolate and ethanolate suggested that two-step desolvation of methanol and ethanol occurred, respectively (Fig. 6). Microscopic observation on the hot-stage proved that methanolate and ethanolate crystals melted slowly and crystallization occurred during the melting process (Figs. 7, 8). Taken together the results of DSC, TGA and hot-stage microscopy, both methanolate and ethanolate were melted with two-step desolvation and a mixture of forms A and B would be crystallized during the melting process. The peak

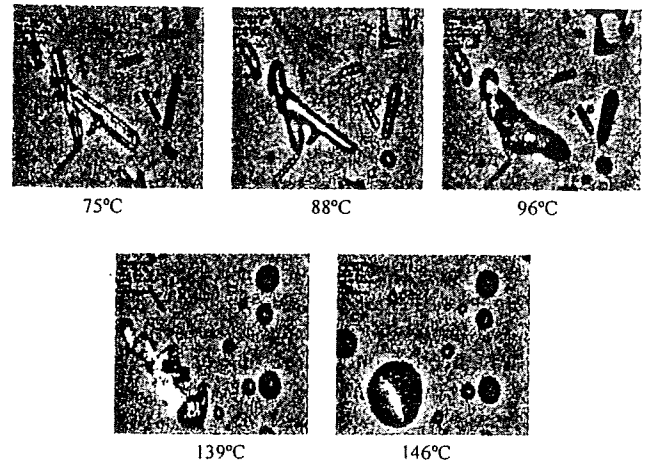

Fig. 7. Polarized Micrographs of Methanolate at Various Temperatures

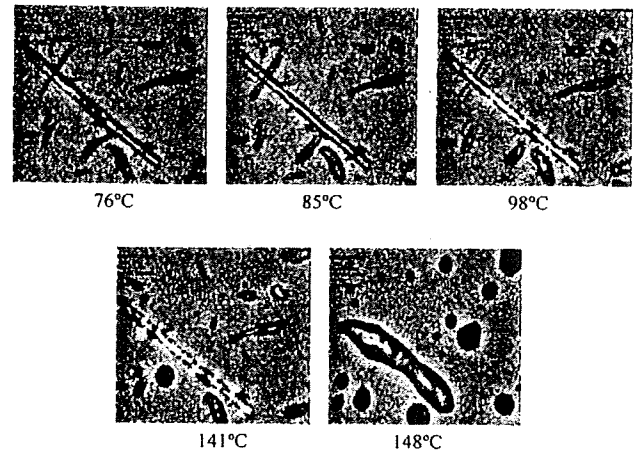

Fig. 8. Polarized Micrographs of Ethanolate at Various Temperatures

area ratio of the melting point of forms A to B on the DSC thermogram for methanolate was lower than that for ethanolate. Furthermore, the results of TGA thermograms of methanolate and ethanolate suggested that 4.9% of methanol and 7.4% of ethanol molecules were included in the crystal entity, respectively. The results of weight loss of these solvates stoichiometrically well corresponded with those of tamoxifen citrate monomethanolate and monoethanolate, which agreed well with the results of single crystal structure analysis.

It was previously reported that form A crystals suspended in ethanol transformed to form B.[24] In their study, the existence of tamoxifen citrate ethanolate was not confirmed even though form A crystals were suspended in ethanol. Based on the results of our thermal analysis of ethanolate, form B crystals in the previous article reported by Goldberg[24] would be observed after desolvation of ethanol from ethanolate and the subsequent transformation from the mixture of forms A and B to the stable form B.

Spectroscopic Analysis Tamoxifen citrate forms A and B, methanolate, and ethanolate were evaluated by diffuse reflectance infrared Fourier-transform spectroscopy (DRIFTS). In the FT-IR spectra, form A showed a sharp band at 1732 cm^{-1} attributable to the stretching of C=O bond of cit-

ric acid, while form B showed a sharp band at 3405 cm^{-1} attributable to the stretching of O–H bond and two strong bands at 1707 and 1740 cm^{-1} attributable to C=O bond of citric acid (Fig. 9). Methanolate showed a broad band at 3250 cm^{-1} attributable to O–H bond, and two strong bands at 1720 and 1695 cm^{-1} attributable to C=O bond of citric acid. Ethanolate also showed a broad band at 3243 cm^{-1} attributable to O–H bond, and two strong bands at 1718 and 1697 cm^{-1} attributable to C=O bond of citric acid, thus indicating quite similar spectroscopic properties to methanolate. Based on the result of single crystal X-ray diffractometry, the O–H and C=O bonds of citric acid were involved in cyclic pairs of hydrogen bond interaction between adjacent citrate species. The differences of wave number in O–H and C=O bonds of citric acid between form B and solvate crystals were consistent with the result of crystal structures which showed different cyclic pairs of hydrogen bonding patterns.

Physicochemical Stability of Polymorphs The physicochemical stability of forms A and B, methanolate and ethanolate was evaluated at 75 and 97% RH at 40 and 60 °C, and the results are summarized in Table 1. Neither form A nor B transformed to each other even under these severe storage conditions, indicating that these forms were quite stable. This is consistent with the results shown in Fig. 5, where no thermal peak due to polymorphic transformation was observed for any of these forms. Methanolate immediately transformed to a crystalline mixture of forms A and B, and subsequently transformed to the stable form B. On the other hand, ethanolate also immediately transformed to the crystalline mixture of forms A and B but no subsequent transformation to the stable form B completely occurred. Taking account of the results of both stability and DSC analysis, it could be said that the amount of stable form B in the crystalline mixture after desolvation of methanolate was more predominant than for ethanolate.

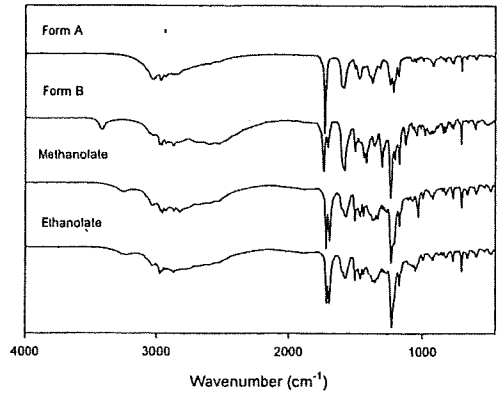

Fig. 9. FT-IR Spectra of Forms A and B, Methanolate and Ethanolate

Conclusion

We have provided for the first time a novel insight into tamoxifen citrate pseudopolymorphs, methanolate and ethanolate. Single crystal X-ray analysis and TGA revealed that the stoichiometry of tamoxifen citrate : methanol and tamoxifen citrate : ethanol was 1 : 1 in any case. The crystal structures of methanolate and ethanolate also revealed that intermolecular interaction between adjacent citrate species was different from that of form B crystals.

We have also demonstrated the physicochemical stability of crystal forms. Form A was quite stable for at least 2 months, whereas methanolate immediately transformed to the crystalline mixture of forms A and B after desolvation, and then changed to the stable form B.

Our investigation on the physicochemical properties of tamoxifen citrate methanolate and ethanolate would also provide useful information for the manufacturing process such as crystallization and drying process, and storage condition of tamoxifen citrate as active pharmaceutical ingredient.

Acknowledgement We wish to thank Dr. Kenji Yoza, Bruker AXS for single crystal X-ray analysis.

References

1) Gould P. L., *Int. J. Pharm.*, **33**, 201—217 (1986).
2) Kojima T., Onoue S., Murase N., Katoh F., Mano T., Matsuda Y., *Pharm. Res.*, **23**, 806—812 (2006).
3) Vishweshwar P., McMahon J. A., Bis J. A., Zaworotko M. J., *J. Pharm. Sci.*, **95**, 499—516 (2006).
4) Aguiar A. J., Krc J., Jr., Kinkel A. W., Samyn J. C., *J. Pharm. Sci.*, **56**, 847—853 (1967).
5) Poole J. W., Owen G., Silverio J., Freyhof J. N., Rosenman S. B., *Curr. Ther. Res. Clin. Exp.*, **10**, 292—303 (1968).
6) Pudipeddi M., Serajuddin A. T., *J. Pharm. Sci.*, **94**, 929—939 (2005).
7) Matsuda Y., Tatsumi E., *Int. J. Pharm.*, **60**, 11—26 (1990).
8) Kato F., Otsuka M., Matsuda Y., *Int. J. Pharm.*, **321**, 18—26 (2006).
9) Otsuka M., Hasegawa H., Matsuda Y., *Chem. Pharm. Bull.*, **45**, 894—898 (1997).

Table 1. The Solid-State Stability of Tamoxifen Citrate Modifications under Various Storage Conditions

Crystal form	Storage condition	Period (d)					
		Initial	3	7	14	28	56
Form A (A)	40 °C/75, 97% RH	A	A	A	A	A	A
	60 °C/75, 97% RH	A	A	A	A	A	A
Form B (B)	40 °C/75, 97% RH	B	B	B	B	B	B
	60 °C/75, 97% RH	B	B	B	B	B	B
Methanolate (M)	40 °C/75% RH	M	A (B)[a]	A (B)[a]	A (B)[a]	A, B	B (A)[b]
	40 °C/97% RH	M	A (B)[a]	A (B)[a]	B (A)[b]	B (A)[b]	B
	60 °C/75% RH	M	B (A)[b]	B	—	—	—
	60 °C/97% RH	M	B (A)[b]	B	—	—	—
Ethanolate (E)	40 °C/75% RH	E	A (B, E)[c]	A (B)[a]	A (B)[a]	A (B)[a]	A (B)[a]
	40 °C/97% RH	E	A (B)[a]	A (B)[a]	A (B)[a]	A (B)[a]	A (B)[a]
	60 °C/75% RH	E	A (B)[a]	A (B)[a]	A (B)[a]	A (B)[a]	A (B)[a]
	60 °C/97% RH	E	A (B)[a]	A (B)[a]	A (B)[a]	A (B)[a]	A (B)[a]

a) Predominantly form A with slight form B. *b*) Predominantly form B with slight form A. *c*) Predominantly form A with slight form B and ethanolate.

10) Sun C., Grant D. J., *Pharm. Res.*, **18**, 274—280 (2001).
11) Yu L. X., Lionberger R. A., Raw A. S., D'Costa R., Wu H., Hussain A. S., *Adv. Drug Deliv. Rev.*, **56**, 349—369 (2004).
12) Otsuka M., Teraoka R., Matsuda Y., *Pharm. Res.*, **8**, 1066—1068 (1991).
13) Otsuka M., Onoe M., Matsuda Y., *Pharm. Res.*, **10**, 577—582 (1993).
14) Bergren M. S., Chao R. S., Meulman P. A., Sarver R. W., Lyster M. A., Havens J. L., Hawley M., *J. Pharm. Sci.*, **85**, 834—841 (1996).
15) Henwood S. Q., Liebenberg W., Tiedt L. R., Lötter A. P., Villiers M. M., *Drug Dev. Ind. Pharm.*, **27**, 1017—1030 (2001).
16) Maurin M. B., Vickery R. D., Rabel S. R., Rowe S. M., Everlof J. G., Nemeth G. A., Campbell G. C., Foris C. M., *J. Pharm. Sci.*, **91**, 2599—2604 (2002).
17) Yoshihashi Y., Yonemochi E., Terada K., *Pharm. Dev. Technol.*, **7**, 89—95 (2002).
18) Chawla G., Gupta P., Thilagavathi R., Chakraborti A. K., Bansal A. K., *Eur. J. Pharm. Sci.*, **20**, 305—317 (2003).
19) Brigger I., Chaminade P., Marsaud V., Appel M., Besnard M., Gurny R., Renoir M., Couvreur P., *Int. J. Pharm.*, **214**, 37—42 (2001).
20) Bhatia A., Kumar R., Katare O. P., *J. Pharm. Pharm. Sci.*, **7**, 252—259 (2004).
21) Ho S., Calder R. J., Thomas C. P., Heard C. M., *J. Pharm. Pharmacol.*, **56**, 1357—1364 (2004).
22) Zeisig R., Ruckerl D., Fichtner I., *Anticancer Drugs*, **15**, 707—714 (2004).
23) Shenoy D. B., Amiji M. M., *Int. J. Pharm.*, **293**, 261—270 (2005).
24) Goldberg I., Becker Y., *J. Pharm. Sci.*, **76**, 259—264 (1987).
25) Kojima T., Onoue S., Katoh F., Teraoka R., Matsuda Y., Kitagawa S., Tsuhako M., *Int. J. Pharm.*, in press.

製剤技術 製剤と粒子設計

医薬品開発における結晶形の効率的選択 —塩・結晶多形スクリーニングへのラマン分光法の応用—

Effective selection of crystal form in pharmaceutical development —Application of Raman spectroscopy to salt and polymorph screenings—

ファイザー株式会社 中央研究所[1]，神戸薬科大学[2]

小嶌隆史[1]，松田芳久[2]

TAKASHI KOJIMA[1]，YOSHIHISA MATSUDA[2]

Pharmaceutical R&D, Science and Technology, Pfizer Global Research and Development, Nagoya Laboratories, Pfizer Japan Inc.[1]
Kobe Pharmaceutical University [2]

Crystal form selection of pharmaceutical compounds including salts, cocrystal and polymorphs is an essential process in the field of drug development. In order to optimize the crystal form, numerous studies dealing with high-throughput salt and polymorph screening on multi-well plates have been conducted. High-throughput salt and polymorph screening is commonly performed by using powder X-ray diffractometory (PXRD) and Raman microscopy. Raman microscopy is especially useful for salt screening, since the technique can provide not only physical information but also chemical information. This review introduces an effective method for salt and polymorph screening by using multi-well plates and Raman microscope, providing information on the stoichiometry of pharmaceutical drug salts obtained. In addition, a case study of pharmaceutical development using salt screening with Raman microscopy is described.

はじめに

市販製剤の原薬や開発段階にある医薬品の大多数は結晶であるが，医薬品は複雑な化学構造を有することから約70%以上が複数の結晶形(結晶多形・擬似多形)をもつことが知られている。個々の結晶形は固有の物理化学的・化学的性質を有することから，固体医薬品の開発において，最適な結晶形を選択し，さらに選択された結晶形の物性を十分に評価しておくことは，合理的な製剤設計を図り，かつ製剤工程を円滑化するために極めて重要である。例えば，医薬品の開発過程における候補化合物の塩や結晶形の種類により，薬物動態や安全性[1,2]だけでなく，製造工程や品質管理面への影響[3~6]等が報告されている。また，医薬品開発において選択した結晶形が不適切であったことに起因する特許訴訟[7]や市販品の製造中止[8]の事例もあり，企業が受けるダメージだけでなく社会に対する影響も大きい。

結晶形選択の重要性は多くの製薬企業で認識されており，ほぼ共通したプロセスの概念(Fig. 1)を持っていると思われる。しかし，実際には結晶形選択を実施している製薬企業にとって社外(学界)における結晶形選択のプロセスや選択された結晶形についての議論は知的財産の観点から困難であることが多い。そのため，短期間かつ低コストを可能とする効率的な結晶形の選択方法および物性評価方法については学界で十分体系的に議論されず，多くの製薬企業では結晶形の選択および物性評価は各社のノウハウに依存した独自のプロセスで行われ，時には非効率的な場合も見受けられる。このため，近年，欧米のベンチャー企業を中心として開発化合物の結晶形選択ツールの販売，受託研究，さらには結晶形選択のコンサルタント業務までがビジネスとなり，活発化している。言うまでもなく，医薬品開発における結晶形の選択を効率的に行うためには，医薬品候補化合物の物性プロファイルとその問題点だけでなく，マーケットの状況，開発コストの予測等の情報も必要であり，科学技術とビジネスの両観点のバランスが重要である。本稿では，結晶形